Eur. Phys. J. D **7**, 379–390 (1999)

THE EUROPEAN PHYSICAL JOURNAL D

EDP Sciences

Condensation of laser cooled gases

L. Santos[1,2] and M. Lewenstein[2,a]

[1] Departamento de Física Aplicada, Universidad de Salamanca, Plaza de la Merced s/n, 37008 Salamanca, Spain
[2] Institut für Theoretische Physik, Universität Hannover, Appelstr. 2, 30167 Hannover, Germany

Received 30 November 1998 and Received in final form 20 March 1999

Abstract. We study a dynamical scheme for condensation of bosonic trapped gases beyond the Lamb-Dicke limit, when the photon-recoil energy is larger than the energy spacing of the trap. Using quantum master equation formalism we demonstrate that dark-state cooling methods similar to those designed for a single trapped atom allow for the condensation of a collection of bosons into a single state of the trap, either the ground, or an excited state. By means of Monte-Carlo simulations we analyse the condensation dynamics for different dimensions, and for different cooling schemes.

PACS. 03.75.Fi Phase coherent atomic ensembles; quantum condensation phenomena – 32.80.Pj Optical cooling of atoms; trapping – 42.50.Vk Mechanical effects of light on atoms, molecules, electrons, and ions

1 Introduction

During the last years the combination of laser-cooling techniques [1] and evaporative [2] or sympathetic cooling [3] has led to the experimental achievement of one of the most pursued goals of quantum physics since its early days, *i.e.* the Bose-Einstein condensation (BEC). However, the question whether BEC is attainable by using all-optical means still remains open, and several experimental groups are investigating this challenging possibility [4–6].

Laser cooling techniques, as Velocity Selective Coherent Population Trapping (VSCPT) [7] or Raman cooling [8], have been designed to cool atomic samples up to fractions of the recoil energy, $E_{\rm R} = \hbar\omega_{\rm R} = \hbar^2 k_{\rm L}^2/2M$, where $k_{\rm L}$ is the laser wavevector and M is the atomic mass. The subrecoil laser cooling methods are based on the very important idea of dark states [9]. These states cannot absorb the laser light, but can receive population *via* incoherent pumping, *i.e. via* spontaneous emission, and therefore these states behave as trapping states. Already designed subrecoil laser cooling techniques should, in principle, lead to the condensation, because in traps of realistic size, *i.e.* larger than $k_{\rm L}^{-1}$, the temperatures needed to achieve condensation are only slightly below, or of the order of $E_{\rm R}$. However, light reabsorption becomes an important difficulty when applying dark-state cooling techniques for high density gases. The dark states, although dark with respect to the laser light, are unfortunately not dark with respect to the photons spontaneously emitted by other atoms, and therefore multiple reabsorptions can increase the system energy by several recoil energies per atom [10–13]. Thus, dark-state techniques cease to work properly at high densities. In particular, laser induced condensation is feasible only if the reabsorbtion probability is smaller than the inverse of the number of motional energy levels accessible *via* the spontaneous emission processes [11].

The problem of reabsorption has aroused great interest in the last years, and several remedies have been recently suggested. It is easy to understand that assuming that the reabsorption cross section for trapped atoms is the same as in free space, *i.e.* $\simeq 1/k_{\rm L}^2$, the reabsorptions should not cause any problem in one dimension, have to be carefully considered in two dimensions, and forbid condensation in three dimensions. Therefore, as the significance of reabsorptions increases with the dimensionality, working with quasi-one- or two-dimensional systems has been proposed as a possible way to reduce the role of reabsorptions. Other suggestion consists in using a strongly confining trap with a frequency $\omega \simeq \omega_{\rm R}$. In this case, as demonstrated in reference [14] for the case of two atom system, the relative role of reabsorption in such a trap can be significantly reduced. It is, however, not clear whether this result would hold for many atom systems. Perhaps the most promising remedy against the reabsorption problem, however, employs the dependence of the reabsorption probability for trapped atoms on the fluorescence rate γ, which can be adjusted at will in dark state cooling [15]. In particular, in the, so called, *Festina Lente* limit, when γ is much smaller than the trap frequency ω [16], the reabsorption processes, in which the atoms change energy and undergo heating, are practically completely suppressed.

In a recent paper [17], following the ideas of reference [18] we have proposed a cooling mechanism (which we have called Dynamical Cooling) which allows for confining of a single trapped atom in one level of the trap,

[a] e-mail: lewen@itp.uni-honnover.de

either the ground or an excited level. The confinement is possible beyond the Lamb-Dicke limit, that is when $E_{\rm R} > \hbar\omega$. The latter condition requires that the so-called Lamb-Dicke parameter $\eta = k_{\rm L} a_0 > 1$ (where $a_0 = \sqrt{(}\hbar/2M\omega)$ is the size of the ground state of the trap). This cooling method is possible because under certain circumstances a particular level of the trap can become a dark-state. We have proposed in [17] two different dark-state mechanisms, one based on the properties of the Franck-Condon factors and the other one (which appears in dimensions higher than one), based on the destructive interference of the amplitudes of absorption of two lasers in orthogonal directions. Dynamical cooling consists in the use of sequences of pulses of different frequencies in such a way that only a desired dark state remains unemptied (dark) during the process, and therefore the population is pumped into this particular level. Typically the use of dark-state (fine-cooling) pulse is not sufficient to achieve the perfect cooling; one has also to use confining pulses (which confine the atomic population to energies of the order of recoil energy), pseudo-confining pulses and auxiliary pulses (that empty the undesired dark states if such appear) (for details see Refs. [17,18]).

In a recent letter [19] we have extended the Dynamical Cooling scheme for the case of N bosonic atoms in the trap. We have presented there a somewhat different cooling scheme than in reference [17] in which the absorption and spontaneous emission processes are considered separately and consecutively, instead of simultaneously as in reference [17]. We have demonstrated that for this model the condensation is possible, and faster and more robust than in the one-atom case.

The aim of this paper is to extend the results of reference [17] to the case in which many atoms are trapped, and also to present in more detail the cooling scheme of reference [19]. The structure of the paper is as follows. In Section 2 we present the Master Equation (ME) which describes the cooling dynamics for the same cooling scheme as that of reference [17], but with many atoms in the trap. In Section 3 we employ adiabatic elimination techniques to obtain a set of rate equations describing level population dynamics, and discuss the quantum-statistical terms appearing in the rates. In Section 4 we solve the rate equations using Monte-Carlo simulations, and study the condensation dynamics into the ground state and into an excited state of the trap in one and two dimensions. In Section 5 the second laser cooling scheme of [19] is presented in detail, and the ME which describes the process is described. In Section 6 we present tridimensional Monte-Carlo simulations of the condensation dynamics for this second model. We finalize in Section 7 with some conclusions.

2 Master equation

We assume in this section the same atomic model as that presented in [17], *i.e.* a three-level Λ-system, composed of a ground-state level $|g\rangle$, a metastable state $|e\rangle$ and an auxiliary third rapidly-decaying state $|r\rangle$. Two lasers excite coherently the resonant Raman transition $|g\rangle \to |e\rangle$ (with some associated effective Rabi frequency Ω), while a repumping laser in or off-resonance with the transition $|g\rangle \to |r\rangle$ pumps optically the atom into $|g\rangle$. With this three level scheme, one obtains an effective two-level system with an effective spontaneous emission rate γ, which can be controlled by varying the intensity, or the detuning of the repumping laser [20].

The main difference respect to [17] is that in this paper we will deal with N identical two-level bosons in the trap, instead of just one. Since even in very dense atomic systems in traps, typical interatomic distances are very large compared with the typical electromagnetic wavefunction size ($\sim$ Bohr radius $r_0 \simeq 5\times 10^{-11}$ m), and since the wavelength of the photons involved in atom-field interaction satisfies $\lambda \gg r_0$, then the atoms keep their bosonic identity in the course of dynamics, and their interaction with photons can be described using the dipole approximation. In order to take into account the quantum-statistical effects which appear in the bosonic collectivity, we need to treat the atoms in second-quantization formalism. We use the approach of "Quantum Field Theory of Atoms and Photons" developed in references [21,22] to describe quantum-statistical systems of cooled and trapped atoms undergoing spontaneous and stimulated emission processes. This theory is in fact quite general, and has been developed also for multicondensate and fermion systems, and for various cases and gauges. We use this theory to write down the appropriate Hamiltonian of the system in question, and to derive the quantum master equation, describing system dynamics after elimination of the electrodynamic degrees of freedom.

In the following we will neglect the atom-atom interactions, *i.e.* we will work in the so-called *Ideal-Gas Approximation*. In principle this approximation implies that we should deal with a small number of particles and/or large traps. However, the s-wave scattering length a (which governs the atom-atom interactions at low energies) can be externally modified [23] by using a magnetic field, and in principle a can be made very close to zero, allowing the strict validity of the ideal gas approximation. We return to this point in Section 7.

Hereafter we consider $\hbar = c = 1$ for simplicity, and follow approximately the notation of [24]. Let us introduce the annihilation and creation operators of atoms in the ground (excited) state and in the trap level m (l), which we will call g_m, $g_m^\dagger$ (e_l, $e_l^\dagger$). These operators fulfill the bosonic commutation relations:

$$[g_m, g_{m'}^\dagger] = \delta_{m,m'}, \tag{1a}$$

$$[e_l, e_{l'}^\dagger] = \delta_{l,l'}. \tag{1b}$$

We use standard quantum-stochastic methods [25–27] to derive the quantum Master Equation (ME) which describes the atomic dynamics (see Appendix A). After tracing over the vacuum electromagnetic modes and under the Born-Markov approximation, the dynamics of the density matrix ρ of the bosonic system is more conveniently described in the interaction picture with respect to the free

atomic Hamiltonian,

$$\hat{H}_{\rm a} = \sum_m \omega^{\rm g}_m g^\dagger_m g_m + \sum_l (\omega^{\rm e}_l + \omega_0) e^\dagger_l e_l, \qquad (2)$$

where the energies of the ground (excited) trap levels are given by $\omega^{\rm g}_m$ ($\omega^{\rm e}_l$). The transition energy between the ground and excited state is given by ω_0. We assume that the center-of-mass potentials for ground and excited atoms can be well approximated by harmonic potentials of frequencies $\omega_{\rm g}$ and $\omega_{\rm e}$, so that $\omega^{\rm g}_m = \omega_{\rm g} m$ and $\omega^{\rm e}_l = \omega_{\rm e} l$. We assume $\gamma < \omega_{\rm g}, \omega_{\rm e}$, *i.e.* we are in the Festina-Lente limit. In this limit rotation-wave approximation (RWA) with respect to trap frequencies will hold. In order to exploit fully the Festina Lente limit, however, it is necessary to assure that the equality of the transition frequencies $\omega^{\rm e}_l - \omega^{\rm g}_m = \omega^{\rm e}_{l'} - \omega^{\rm g}_{m'}$ implies $m = m'$ and $l = l'$. This can be achieved in two ways: (i) one can consider $\omega_{\rm g} = \omega_{\rm e} = \omega$ but introduce a small anharmonicity in the ground state potential, so that $\omega^{\rm g}_m = \omega_m + \omega\alpha m^2$, with $\alpha \ll 1$. In this case γ must be smaller than $\alpha\omega$ [28]; (ii) other possibility employs two incommensurable frequencies $\omega_{\rm g} \neq \omega_{\rm e}$. In this case γ has to be smaller than $|\omega_{\rm e} - \omega_{\rm g}|$. This second possibility is easy to realise in magnetic and optical traps. Both mentioned conditions assure that there are strictly speaking no degenerated transition frequencies. In both cases there may occur quasi-degeneracies, but they will typically happen for large l, l', m, m' and will not play significant role in the dynamics. Obviously the above considerations can be extended to higher dimensions, where we replace the quantum number m, l, by the corresponding pairs, or triples of quantum numbers. In higher dimensions it is recommended to use asymmetric harmonic potentials, with incommensurable frequencies in all directions [15].

The quantum master equation takes the following form:

$$\begin{aligned}\dot{\tilde{\rho}}(t) = &-{\rm i}[\tilde{H}_{\rm las}(t), \tilde{\rho}(t)] + \gamma \sum_{m,m',l,l'} {\rm e}^{{\rm i}(\Delta_{lm} - \Delta_{l'm'})t} \xi_{lmm'l'}(\omega_0) \\ &\times [2\tilde{g}^\dagger_{m'} \tilde{e}_{l'} \tilde{\rho}(t) \tilde{e}^\dagger_l \tilde{g}_m - \tilde{e}^\dagger_l \tilde{g}_m \tilde{g}^\dagger_{m'} \tilde{e}_{l'} \tilde{\rho}(t) - \tilde{\rho}(t) \tilde{e}^\dagger_l \tilde{g}_m \tilde{g}^\dagger_{m'} \tilde{e}_{l'}] \\ &- {\rm i} \sum_{m,m',l,l'} \Delta_{lmm'l'} {\rm e}^{{\rm i}(\Delta_{lm} - \Delta_{l'm'})t} [\tilde{e}^\dagger_m \tilde{g}_l \tilde{g}^\dagger_{l'} \tilde{g}^\dagger_{l'} \tilde{e}_{m'}, \tilde{\rho}(t)], \end{aligned} \qquad (3)$$

with

$$\xi_{lmm'l'}(k) = \int {\rm d}\phi {\rm d}\theta \sin\theta \mathcal{W}(\theta, \phi) \eta_{lm}(\mathbf{k}) \eta^*_{l'm'}(\mathbf{k}), \qquad (4)$$

$$\Delta_{lmm'l'} = \frac{\gamma}{\pi} \mathcal{P} \int_{-\infty}^{\infty} {\rm d}u \frac{u^3}{u-1} \xi^*_{lmm'l'}(u\omega_0), \qquad (5)$$

where $\eta_{lm}(\mathbf{k}) = \langle e, l | {\rm e}^{{\rm i}\mathbf{k}\cdot\mathbf{r}} | g, m \rangle$ are the Franck-Condon factors, $\mathcal{W}(\theta, \phi)$ is the fluorescence dipole pattern, $\Delta_{lm} = \omega^{\rm e}_l - \omega^{\rm g}_m$, and 2γ is the single-atom spontaneous emission rate. Note that for standard dipole transitions $\gamma = (d^2\omega_0^3)/(16\epsilon_0\pi^2)$, where d is the dipole matrix element of the corresponding transition. For the spontaneous Raman transition from the level $|g\rangle$ to $|e\rangle$ *via* $|r\rangle$, the effective $\gamma \propto \gamma_{\rm re}\Omega^2_{\rm gr}/(\Delta^2_{\rm gr} + \gamma^2_{\rm re})$, where $2\gamma_{\rm re}$ is the spontaneous emission rate from $|r\rangle$ to $|e\rangle$, while $\Omega_{\rm gr}$ and $\Delta_{\rm gr}$ denote the laser Rabi frequency and detuning of the transition $|g\rangle \to |r\rangle$, respectively. In equation (5) $\mathcal{P}$ indicates the Cauchy Principal Part of the integral, and finally

$$\tilde{H}_{\rm las} = \frac{\Omega}{2} \sum_{l,m} \eta_{lm}(k_{\rm L}) {\rm e}^{-{\rm i}(\delta - (\omega^{\rm e}_l - \omega^{\rm g}_m))t} \tilde{e}^\dagger_l \tilde{g}_m + h.c., \qquad (6)$$

is the atom-laser interaction Hamiltonian in the interaction picture with $\hat{H}_{\rm a}$.

Writing the ME in the frame rotating with the laser frequency:

$$\dot{\rho}(t) = -{\rm i}[\hat{H}_{\rm a} + \hat{H}_{\rm las} + \sum_{ll'} \Delta_{lmml'} e^\dagger_l e_{l'} + \hat{H}_{\rm dip}, \rho(t)] + \mathcal{L}\rho(t) \qquad (7)$$

where:

$$\hat{H}_{\rm a} = \sum_m \omega^{\rm g}_m g^\dagger_m g_m + \sum_l (\omega^{\rm e}_l - \delta) e^\dagger_l e_l, \qquad (8)$$

$$\hat{H}_{\rm las} = \frac{\Omega}{2} \sum_{l,m} \eta_{lm}(k_{\rm L}) e^\dagger_l g_m + h.c., \qquad (9)$$

$$\hat{H}_{\rm dip} = \sum_{m,m',l,l'} \Delta_{lmm'l'} e^\dagger_l g^\dagger_{m'} g_m e_{l'}, \qquad (10)$$

$$\begin{aligned}\mathcal{L}\rho(t) = \gamma \sum_{m,m',l,l'} &\xi_{lmm'l'}(\omega_0) [2 g^\dagger_{m'} e_{l'} \rho(t) e^\dagger_l g_m \\ &- e^\dagger_l g_m g^\dagger_{m'} e_{l'} \rho(t) - \rho(t) e^\dagger_l g_m g^\dagger_{m'} e_{l'}]. \end{aligned} \qquad (11)$$

Using the fact that we consider Festina Lente limit we can apply RWA, and neglect the terms such that $\Delta_{ml} \neq \Delta_{m'l'}$. Moreover, due to the assumed form of the ground and excited state potentials (see the discussion after Eq. (2)), in the RWA only the terms with $m = m'$, $l = l'$ survive. Neglecting $\hat{H}_{\rm dip}$ which describes the dipole-dipole interactions between ground and excited atoms, and absorbing the single-atom Lamb-shift $\sum_l \Delta_{lmml} e^\dagger_l e_l$ into ω_0, we finally obtain:

$$\dot{\rho}(t) = -{\rm i}\hat{H}_{\rm eff}\rho(t) + {\rm i}\rho(t)\hat{H}^\dagger_{\rm eff} + \mathcal{J}\rho(t) - {\rm i}[\hat{H}_{\rm las}, \rho(t)], \qquad (12)$$

where the effective (non-Hermitian) Hamiltonian is of the form:

$$\hat{H}_{\rm eff} = \hat{H}_{\rm a} - {\rm i}\gamma \int {\rm d}\phi {\rm d}\theta \sin\theta \mathcal{W}(\theta, \phi) \sum_{l,m} |\eta_{lm}(\mathbf{k})|^2 e^\dagger_l g_m g^\dagger_m e_l, \qquad (13)$$

and the jump superoperator is:

$$\begin{aligned}\mathcal{J}\rho(t) = 2\gamma &\int {\rm d}\phi {\rm d}\theta \sin\theta \mathcal{W}(\theta, \phi) \\ &\times \sum_{l,m} [\eta^*_{lm}(\mathbf{k}) g^\dagger_m e_l] \rho(t) [\eta_{lm}(\mathbf{k}) e^\dagger_l g_m]. \end{aligned} \qquad (14)$$

One should stress here that the neglection of $\hat{H}_{\rm dip}$ is strictly speaking possible when the optical parameter

$n/k^3 < 1$ (where n is the atomic density). When $n/k^3 \simeq 1$, both $\hat{H}_{\rm dip}$, and the two-atom part of $\hat{H}_{\rm eff}$ are of the same order. It is worth stressing that the contribution of $\hat{H}_{\rm dip}$ cancels *exactly* in the second kind of master equation discussed in Section 5. Neglection of $\hat{H}_{\rm dip}$ permits thus a more direct comparison of the models, and therefore in most of the calculations of Section 4 we will thus neglect $\hat{H}_{\rm dip}$. Nevertheless, in order to illustrate possible effects of $\hat{H}_{\rm dip}$ we shall present in Section 4 some numerical results including $\hat{H}_{\rm dip}$ term. Within the RWA the inclusion of $\hat{H}_{\rm dip}$ (as a real part of $\hat{H}_{\rm eff}$) is straightforward, but technically complicated because it involves the calculation of the Cauchy principal parts of the integrals for the matrix elements $\Delta_{lmm'l'}$.

One should note that the master equation in the Festina Lente limit has a quite different form than master equations obtained beyond that limit. In particular, in the considered limit, and for an ideal gas, there is no need to treat the master equation self-consistently. This is a big difference in comparison to Hartree-Fock treatments developed by Meystre's group (see for instance Ref. [29]) to describe nonlinear atom optics and atom laser. In this sense Festina Lente limit provides very essential simplifications. In particular, in our case no modifications of the ground state wave function due to dipole-dipole interactions are expected to occur. Festina Lente limit is the limit of weak electromagnetic interactions ($\gamma \ll \omega$), which can be achieved either for forbidden transitions, or for far detuned Raman transitions. Within the RWA implied by Festina Lente limit ground state wave function is not modified. The corrections appear first in higher orders of the Festina Lente expansion parameters. Moreover, in order to have such corrections, the laser should partially excite a large number of atoms. As we shall see in the next section this is not the case in our scheme.

3 Adiabatic elimination of the excited state. Rate equations

In the regime of parameters considered, most of the atoms are in the ground state during the dynamics. In particular the system is characterized by two different time scales: a slow one, given by the commutator with $\hat{H}_{\rm las}$ in the RHS of equation (12), and the faster one given by the rest of the RHS. Thanks to this time-scale separation we can use adiabatic elimination techniques to remove the excited-state populations. By using standard Projection Operator techniques it is possible to show that the adiabatic elimination of the excited state levels leads to a set of rate equations for the populations N_m of each level of the ground-state trap:

$$\dot{N}_n = \sum_m \Gamma_{n\leftarrow m} N_m - \sum_m \Gamma_{m\leftarrow n} N_n, \qquad (15)$$

where the rates of populating level $|n\rangle$ by transitions from the level $|m\rangle$ are of the form:

$$\Gamma_{n\leftarrow m} = \frac{\Omega^2}{2\gamma}\int_0^{2\pi} \mathrm{d}\phi \int_0^{\pi} \mathrm{d}\theta \mathcal{W}(\theta,\phi) \times \left| \sum_l \frac{\gamma \eta^*_{ln}(\mathbf{k})\eta_{lm}(k_{\rm L})}{[\delta - \omega(l-m)] + \mathrm{i}\gamma R_{ml}} \right|^2 (N_n + 1 - \delta_{n,m}). \qquad (16)$$

In the above expressions we have approximated the excited and ground potentials by identical isotropic harmonic potentials of frequency ω, and denoted

$$R_{ml} = \int_0^{2\pi} \mathrm{d}\phi \int_0^{\pi} \mathrm{d}\theta \mathcal{W}(\theta,\phi) \times \sum_{n'} |\eta_{ln'}(\mathbf{k})|^2 (N_{n'} + 1 - \delta_{n',m}). \qquad (17)$$

In the above expressions $\delta_{n,m}$ denotes a Kronecker delta, and physically accounts for the fact that an autotransition from n to n can also occur, but its probability is proportional to the occupation of the final state N_n, rather than to $N_n + 1$ which is characteristic for m to n transitions with $m \neq n$.

Note that the rates (16) and the single-atom ones of reference [17] are quite different. In the single-atom case, the rates (16) coincide with those of reference [17] as they should, but for the many-atom case, the rates (16) become nonlinear, due to their dependence on the number of atoms in each trap level. In particular, two different quantum-statistical contributions can be noticed:

- in the denominator of the rates, the spontaneous emission acquires a collective character (similar as that observed in superradiance [30]). That, of course, implies that the validity of the Festina Lente limit requires that the collective rates are smaller than the trap frequency;
- in the numerator of the rates, the bosonic-enhancement factor $(N_n + 1 - \delta_{n,m})$ appears.

The contribution of the bosonic-enhancement factor is quite interesting since it favors the condensation of atoms into just one level of the trap. The reason is that if we are able to pump a significant amount of atoms into one single level $|n\rangle$, subsequent transitions into $|n\rangle$ are more and more probable.

The contribution of the collective spontaneous emission is unfortunately not so advantageous. The cooling methods designed for the single-atom case, which we want to apply in the many-atom case, are based on resonant processes, and are therefore quite dependent on a narrow resonance. Note that the width of the resonance centered at $\delta = \omega(l-m)$ is given by γR_{ml}. If γR_{ml} grows, then the resonance is broadened, and the dark-state effects could cease to exist. On the other hand, as R_{ml} grows, the height of the resonance becomes lower, and consequently the cooling becomes slower.

These negative effects can be avoided by using a sufficiently small γ. In the following we will consider

$\gamma = 0.005\omega$ in all the calculations, which guarantees in the worst case (one-dimensional calculations) that only the resonant terms are relevant. We will show in the next section that the negative effects are less important for higher dimensions. Note, however, that the decreasing of γ makes also the cooling slower. For some of the following examples, the choice of γ leads to very large cooling times (larger than 20 seconds for sodium atoms). This technical problem, however, can be eventually solved by decreasing gradually γ during the cooling process, in such a way that the maximum effective collective spontaneous emission rate remains approximately constant. Such optimization would increase the cooling rate, allowing realistic cooling times.

4 Results

In the following we simulate numerically rate equations (15) using standard Monte-Carlo methods. We will consider in this section the case of $N = 500$ atoms, and, if otherwise not indicated, the value $\eta = 3.00$. All of the calculations in this section have been performed with 20 energy shells (*i.e.* 20 levels in one dimension, and 231 levels in two dimensions). In several cases we have also performed the calculations with 30 energy shells, obtaining essentially the same results as for the case of 20 shells. It is easy to observe from the form of the rates (16), and following the same arguments as those used in [17], that as in the single-atom case two different dark-state mechanisms can be designed:

- "Franck-Condon"-dark-states. Let us assume a laser pulse with detuning $\delta = s\omega$ respect to the atomic transition, where s is an integer number. It can be easily proved [17] that a particular level of the trap $|m\rangle$ remains unemptied (dark) if the Franck-Condon factor $\langle m+s|\exp(\mathrm{i}kx)|m\rangle$ vanishes. From the form of such factors, it is easy to demonstrate that the dark-state conditions for $m = 1$ and $m = 2$ are, respectively,

$$\eta^2 = s + 1, \tag{18}$$

$$\eta^2 = (s+2)(1 \pm (s+2)^{-1/2}); \tag{19}$$

- "interference"-dark-states. This dark-state mechanism is characteristic for dimensions higher than one. Let us assume the two-dimensional problem, in which we have two orthogonal lasers characterised by two different Rabi frequencies: Ω in direction x, and $A\Omega$ in direction y. The complex factor A indicates a possible difference between the intensities and/or phases of both lasers, and can be used to develop a dark-state mechanism. If the laser detuning is zero, selecting a particular two-dimensional state $|m_x^0, m_y^0\rangle$, and choosing the value $A = -\langle m_x^0|\mathrm{e}^{\mathrm{i}kx}|m_x^0\rangle/\langle m_y^0|\mathrm{e}^{\mathrm{i}ky}|m_y^0\rangle$, it can be proved that the selected level remains dark respect to the laser pulse [17].

We will use these dark-state mechanisms to obtain condensation not only into the ground state, but also into an excited state of the trap.

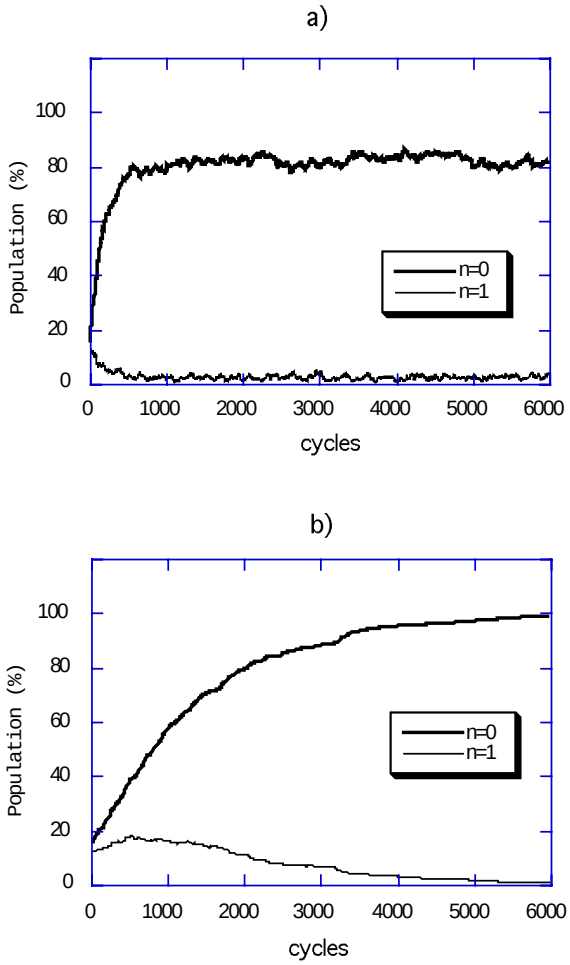

Fig. 1. Population dynamics of $n = 0$ and $n = 1$, using a sequence of pulses of detunings $s = -9$, 0, -10, 1, all of them with duration $2\gamma/\Omega^2$. The Lamb-Dicke parameter is $\eta = 3$. The initial distribution is thermal with mean $\langle n\rangle = 6$. In (a) $N = 1$ is considered whereas in (b) the case of $N = 500$ atoms is depicted.

4.1 Ground state cooling

Let us first analyse the one-dimensional case, *i.e.* the condensation into $n = 0$. In Figure 1 we use a sequence of pulses with detunings $\delta = s\omega$, $s = -9$, 0, -10, 1, and all of them with the duration $T = 2\gamma/\Omega^2$. Pulses 1 and 3 are confining pulses, and 2 and 4 are fine-cooling pulses [17]. Figure 1a shows the dynamics for $N = 1$ for $n = 0$ and 1, whereas Figure 1b shows the case of 500 atoms. Two aspects become clear:

- for this particular sequence, cooling is more effective ($\simeq 100\%$) in the many-atom rather than in the single-atom case ($\simeq 80\%$);
- levels $n = 0$ and $n = 1$ compete in the many atom case. This is due to two facts: first, the level $n = 1$ is not efficiently emptied, because the Lamb-Dicke parameter is quite large [18]; second, the non-linearity tends to populate initially also the level $n = 1$, due to its initially large population. Therefore we observe

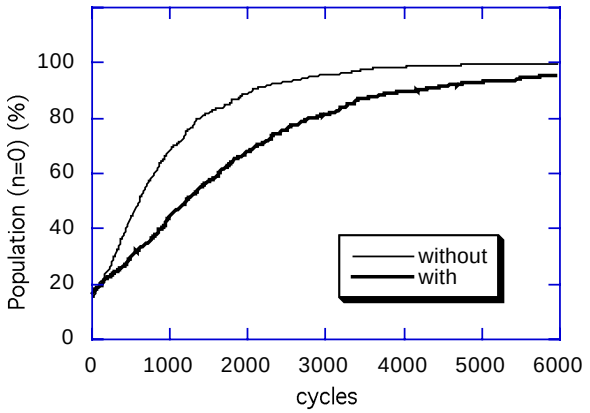

Fig. 2. Population dynamics of $n = 0$ using a sequence of pulses of detunings $s = -9$, 0, -10, -1, all of them with duration $2\gamma/\Omega^2$. The Lamb-Dicke parameter is $\eta = 3$. The initial distribution is thermal with mean $\langle n \rangle = 6$. The cases with and without considering the dipole-dipole shift are depicted.

that the population of $n = 1$ survives during quite a long time, being slowly transferred into $n = 0$.

In Figure 2 we have included the effects of $\hat{H}_{\rm dip}$ as discussed in Section 2. We consider the same sequence of pulses as in Figure 1. The inclusion of the dipole-dipole term clearly slows the one-dimensional condensation. The reason is clear, because the detuning in equation (16) must be substituted by:

$$\delta_{\rm eff} = \delta - \gamma S_{ml}, \tag{20}$$

where

$$S_{ml} = \sum_{n'} \left[\frac{1}{\pi} \mathrm{P} \int_{-\infty}^{\infty} \mathrm{d}u \frac{u^3}{u-1} \xi^*_{lmml}(u\omega_0) \right] (N_{n'} + 1 - \delta_{m,n'}), \tag{21}$$

and therefore the detuning changes during the condensation process, moving apart from the proper detuning values. Nevertheless the condensation is still effective (almost 100%).

Let us analyse now the two-dimensional case, *i.e.* the condensation into $(0,0)$. Let us use the sequence $s = -18$, -9, -4, 0, -19, -10, -5, -1. For all the pulses we consider a duration $T = 2\gamma/\Omega^2$. Pulses 1 and 5 are confinement pulses. Pulse 4 is the dark-state pulse (if $A = -1$). Pulse 8 is the Sideband Cooling pulse. Pulses 2, 3, 6 and 7 are pseudo-confinement pulses [17]. Remember that A denotes the relation between the amplitude of the laser in direction y and the laser in direction x. In Figure 3 we analyse the cases of $A = -1$ and $A = 1$ for $N = 500$ (Fig. 3a) and $N = 1$ (Fig. 3b). Note that

- the case of $A = 1$ for which the single atom cooling is inefficient, becomes quite efficient for 500 atoms, basically due to the bosonic-enhancement;
- unfortunately, the bosonic enhancement does not act only in a positive sense. Note that for $A = -1$, pulse 4 is not only a dark-state pulse for the state $(0,0)$, but also for any state (m,m), and in particular for $(1,1)$.

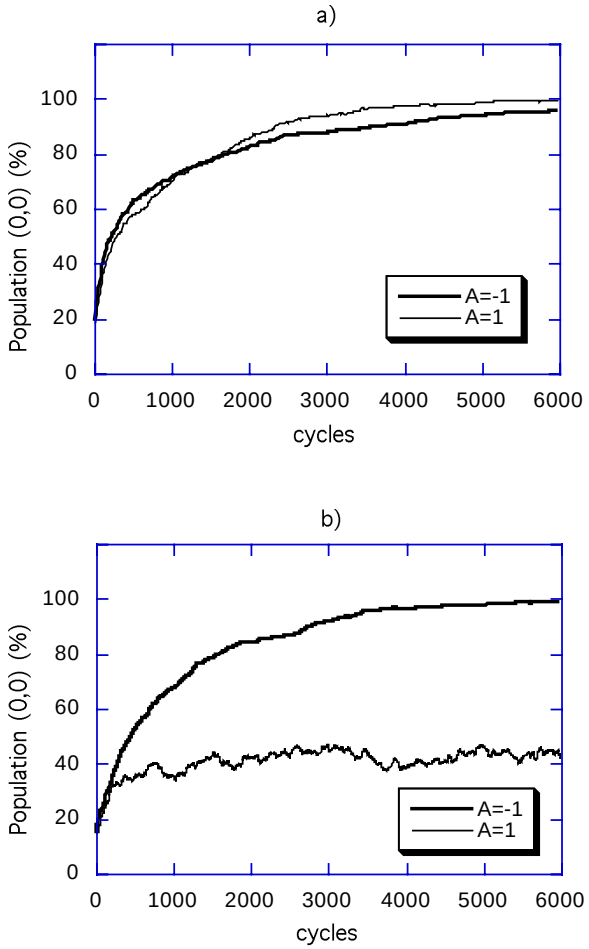

Fig. 3. Population dynamics of $(0,0)$, using a sequence of pulses of detunings $s = -18$, -9, -4, 0, -19, -10, -5, -1, all of them with duration $2\gamma/\Omega^2$. The Lamb-Dicke parameter is $\eta = 3$. The initial distribution is thermal with mean $\langle n \rangle = 6$. In (a) the case of $N = 500$ is depicted for the case in which all the pulses are considered with $A = -1$, and $A = 1$. In (b) the same case as in (a) is presented, but for $N = 1$. $N = 1$ and $N = 500$ are compared.

Also pulse 8 is not efficient enough to empty $(1,1)$ for the considered Lamb-Dicke parameter $\eta = 3$ [18]. Therefore, $(1,1)$ is very slowly transferred to $(0,0)$, and in fact increases its population during the early stages of the cooling process. This slows the condensation into $(1,1)$, and, in fact, the condensation for $A = -1$ is not faster than for $A = 1$. In fact, the latter is more efficient, because although $(0,0)$ is not a dark-state, $(1,1)$ is not too, and the bosonic enhancement favors the condensation into $(0,0)$ more clearly than for $A = -1$. This is one example of a cooling scheme which is efficient for $N = 500$ and not for $N = 1$;

- for the two dimensional case the negative effects of collective spontaneous emission and statistical change of the detuning are negligible. We explain this in more detail in Section 4.2

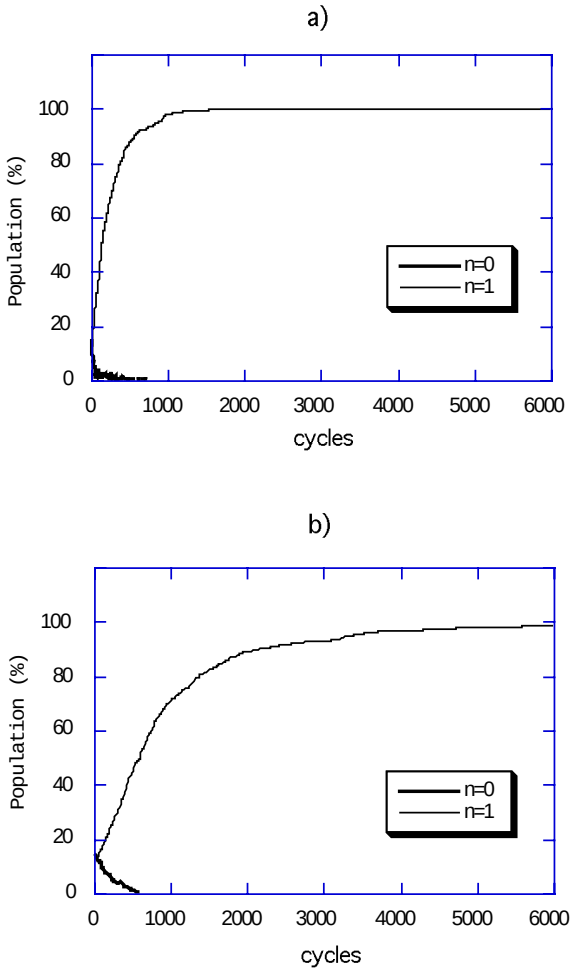

Fig. 4. Population dynamics of $n = 0$ and $n = 1$, using a sequence of pulses of detunings $s = -9, 8, -10, -3$, all of them with duration $2\gamma/\Omega^2$. The Lamb-Dicke parameter is $\eta = 3$. The initial distribution is thermal with mean $\langle n \rangle = 6$. In (a) $N = 1$ is considered whereas in (b) the case of $N = 500$ atoms is depicted.

4.2 Excited-state cooling

As the first example of excited-state cooling let us consider the one-dimensional case of the condensation into $n = 1$. We use the sequence $s = -9, 8, -10, -3$, all of them with a duration $T = 2\gamma/\Omega^2$. Pulses 1 and 3 are confinement pulses, pulse 2 fulfills equation (18), and is therefore the dark-state pulse for the level $|1\rangle$, and pulse 4 is an auxiliary pulse [17]. Figure 4a shows the cooling dynamics for $N = 1$, whereas in Figure 4b we depict the case of $N = 500$. Observe that, contrary to the ground-state cooling, level $n = 0$ is very efficiently emptied (by $s = 8$ pulse). The difference of population of levels $n = 0$ and $n = 1$ is not enough to provide a bosonic-enhancement factor able to counterbalance this efficient emptying, and therefore no relevant many-atom competition is present in this case. Note, however, that $n = 0$ is emptied more slowly for $N = 500$ than for $N = 1$. This effect delays slightly the condensation for the first cycles, but it is not the main

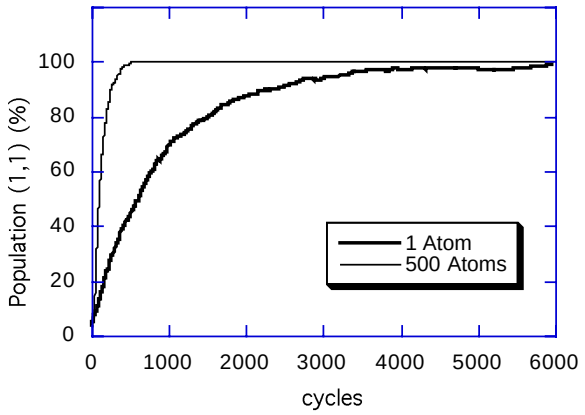

Fig. 5. Population dynamics of $(1, 1)$, using a sequence of pulses of detunings $s = -18, -9, -4, 8, -19, -10, -5, -3$, all of them with duration $2\gamma/\Omega^2$. The Lamb-Dicke parameter is $\eta = 3$. The initial distribution is thermal with mean $\langle n \rangle = 6$. The cases of $N = 1$ and $N = 500$ are compared.

cause of the fact that for this case the many-atom cooling is slower than for $N = 1$. The main cause is the reduction of the height of the resonant peak due to the collective spontaneous emission in the denominator of the rates; as pointed out previously, it makes the cooling slower. This reduction in the denominator can be easily estimated by considering the maximum factor R_{ml} (17):

$$R_{ml}^{\max} \sim \int_0^{2\pi} \mathrm{d}\phi \int_0^{\pi} \mathrm{d}\theta \mathcal{W}(\theta, \phi) |\eta_{l n_0'}(\mathbf{k})|^2 (N + 1 - \delta_{n',m}), \tag{22}$$

where n_0' is the condensed state. The maximum value of expression (22) is for this case 0.48. Therefore, although the resonant term is still the only relevant, the height of the resonant peak is now reduced considerably.

Let us consider the two-dimensional case of the condensation into $(1, 1)$. We use a sequence $s = -18, -9, -4, 8, -19, -10, -5, -3$, all of them with duration $T = 2\gamma/\Omega^2$. Pulses 1 and 5 are confinement pulses, and pulses 2, 3, 6 and 7 are pseudo-confinement pulses. Pulse 4 fulfills equation (18), and it is trivial to see that for an isotropic trap the level $(1, 1)$ of the trap becomes a dark-state for this pulse. Finally pulse 8 avoid the formation of undesired unemptied states. Figure 5 shows the condensation dynamics into $(1, 1)$ for $N = 1$ and $N = 500$ atoms. Observe that contrary to the one-dimensional condensation into $n = 1$, the many-atom cooling is now much faster than for $N = 1$. The reason can be explained by analyzing the terms describing the collective spontaneous emission. Estimating as previously the maximum factor R_{ml}:

$$R_{ml}^{\max} \sim \int_0^{2\pi} \mathrm{d}\phi \int_0^{\pi} \mathrm{d}\theta \mathcal{W}(\theta, \phi) |\eta_{l_x n'_{x,0}}(\mathbf{k})|^2 |\eta_{l_y n'_{y,0}}(\mathbf{k})|^2 \times (N + 1 - \delta_{n_0',m}), \tag{23}$$

we observe the appearance of two Franck-Condon factors instead of just one. This makes the maximum factor (23) very much smaller than in one dimension. In particular

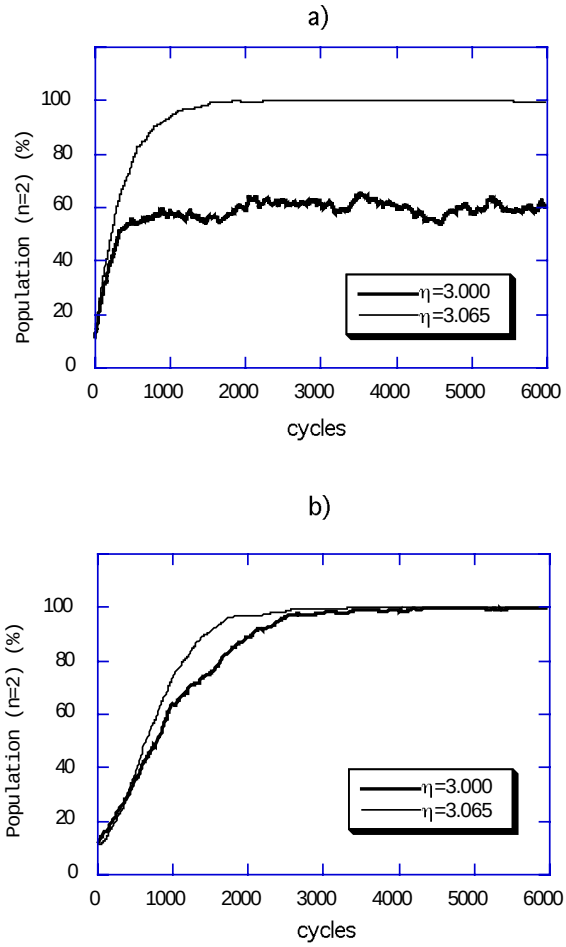

Fig. 6. Population dynamics of $n = 2$, using a sequence of pulses of detunings $s = -9$, 11, -10, -5, all of them with duration $2\gamma/\Omega^2$. Two different Lamb-Dicke parameters $\eta = 3$ and 3.065 are considered. The initial distribution is thermal with mean $\langle n\rangle = 6$. In (a) $N = 1$ is considered whereas in (b) the case of $N = 500$ atoms is depicted. Observe that the cooling for $N = 500$ is more robust than for $N = 1$.

for this case the maximum value is 0.048, *i.e.* ten times lower than for $n = 1$ case. This fact allows for a much rapid condensation into $(1, 1)$, and explains also why the condensation into $(0, 0)$ in Section 4.1 (Fig. 3) is quicker for the many-atom case. This effect also makes for the considered parameters the dipole-dipole shifts negligible for dimensions higher than one.

Finally, let us present an example which clearly illustrates the robustness of the many-atom "Franck-Condon"-dark-state cooling, with respect to the one-atom case. Let us consider the one-dimensional cooling into $n = 2$, using a sequence $s = -9$, 11, -10, -5, all of them with duration $T = 2\gamma/\Omega^2$. The pulses have the same function as for the $n = 1$ cooling case. In particular for $\eta = 3.065$ $s = 11$ satisfies condition (19), and therefore is a "Franck-Condon"-dark-state pulse for $n = 2$. Figure 6 shows the population dynamics of $n = 2$, for the case of $\eta = 3$ and $\eta = 3.065$. In Figure 6a we depict the case of $N = 1$, proving that a slight deviation from the dark-state condition prevents the condensation. Figure 6b shows the case of $N = 500$, and proves that in the many-atom case it is not necessary to fulfill exactly the dark-state condition to achieve the condensation into $n = 2$. *Id est*, the many-atom cooling is (due to the bosonic-enhancement) certainly much more robust and less restrictive than the one-atom cooling.

5 Two-step model

In this section we present a different model of cooling than that of reference [17] and that of the first sections of this paper. Remember that our cooling scheme consists in the absorption of a sequence of pulses (strictly speaking a pair of Raman pulses). The effective spontaneous emission is the result of a spontaneous Raman processes which extract the population of the excited state using a virtual transition through a third rapidly-decaying level. So far both processes (absorption plus spontaneous emission) have been considered simultaneously. In the present section we study the case in which both processes are considered separately and consecutively. *Id est*, the atom is affected by:

- stimulated absorption laser pulses, which induce energy-selective transitions $|g\rangle \to |e\rangle$, depopulating all motional states except the "dark" ones;
- spontaneous emission pulses, which are non-selective, and repump in a, more or less, uniform way all atoms into all the accessible motional states.

As in the previous model we are going to demonstrate that:

- the laser induced condensation into an arbitrary trap level is possible; *i.e.* an arbitrary trap level may be made dark;
- the condensation is robust with respect to changes of physical parameters; dark states do not have to be completely dark.

The new model has advantages with respect to the previous one. In particular, one can avoid the problem of the broadening of the absorption resonance due to the collective spontaneous emission in the new model. This model has also the advantage that the dipole-dipole contribution cancels out exactly. Computationally it presents also advantages, allowing the analysis of three-dimensional problems. Last, but not least, it corresponds well to experiments.

The model and notation is exactly the same as previously. We use the coarse graining in time, and describe the variations of the density matrix after one absorption and one spontaneous emission pulse. After such cooling cycle all atoms are in the ground internal state described by the density matrix $\rho(t)$. This matrix is diagonal in the Fock representation corresponding to the bare trap levels.

We assume the absorption pulses of duration $\tau_{\rm abs}$ are weak and do not excite many atoms. Their effects can thus be described by the second order perturbation theory (formally that corresponds to one atom excited at most). In the absorption step, the dynamics is described

by the simple von Neumann equation (in interaction picture with respect to $\hat{H}_{\rm a}$):

$$\dot{\rho}(t) = -{\rm i}[\hat{H}_{\rm las}(t), \rho(t)], \tag{24}$$

where

$$\hat{H}_{\rm las}(t) = \frac{\Omega(t)}{2} \sum_{l,m} \eta_{lm}(k_{\rm L}) {\rm e}^{-{\rm i}\omega_{\rm L} t} e_l^\dagger g_m + h.c. \tag{25}$$

with $\Omega(t) = \Omega_0 f(t)$, where Ω_0 is the maximal effective Rabi frequency, and $f(t)$ is a temporal envelope of the pulse. Integrating in time, and iterating up to terms of the second order with respect to the laser, we obtain:

$$\rho(t+\tau_{\rm abs}) \simeq \rho(t) - \frac{1}{2}\big[H_{\rm las}, [H_{\rm las}, \rho(t)]\big] \tag{26}$$

In equation (26) we have neglected the first-order terms respect to the laser, because they decay to zero during the spontaneous emission step (that is simple to understand because the corresponding terms lead to off-diagonal matrix elements between the states with one excited and no excited atoms). Also, in equation (26) we have extended the integrals from $-\infty$ to $+\infty$ because the absorption pulse acts only during the interval $\tau_{\rm abs}$; therefore, we find:

$$H_{\rm las} = \frac{\Omega_0}{2} \sum_{l,m} \eta_{lm}(k_{\rm L}) \tilde{f}(\delta - \omega_l^{\rm e} + \omega_m^{\rm g}) e_l^\dagger g_m + h.c. \tag{27}$$

where $\tilde{f}(\delta)$ is the Fourier transform of $f(t)$, which is a function peaked at $\delta = 0$ with a width $\Delta\delta$ of the order of $\tau_{\rm abs}^{-1}$. We can consider, for example, Gaussian pulses of the form $f(t) = \exp(-t^2/\tau_{\rm abs}^2)$. We will assume in the following $\tau_{\rm abs}$ such that the width $\Delta\delta$ of $\tilde{f}$ is smaller than ω. Using this last assumption and the fact that the jump operator (14) is purely diagonal in the l index (and therefore we can neglect the coherences between different excited states, because they do no contribute to the spontaneous emission process), we obtain:

$$\rho(t+\tau_{\rm abs}) = \rho(t) - \sum_{l,m} \Gamma_{lm}^{\rm abs} [g_m^\dagger g_m \rho(t) + \rho(t) g_m^\dagger g_m - 2 e_l^\dagger g_m \rho(t) g_m^\dagger e_l], \tag{28}$$

where

$$\Gamma_{lm}^{\rm abs} = \frac{\Omega_0^2}{8} |\eta_{lm}(k_{\rm L})|^2 |\tilde{f}(\delta - \omega_l^{\rm e} + \omega_m^{\rm g})|^2 \tag{29}$$

are the absorption probabilities, which describe the transitions from the ground state level m to the excited state level l.

The spontaneous emission step is regulated by the ME given by equation (12), but without laser, *i.e.*:

$$\dot{\rho}(t) = -{\rm i}\hat{H}_{\rm eff}\rho(t) + {\rm i}\rho(t)\hat{H}_{\rm eff}^\dagger + \mathcal{J}\rho(t), \tag{30}$$

with

$$\hat{H}_{\rm eff} = -{\rm i} \sum_{l,n} \Gamma_{nl}^{\rm sp} e_l g_n \rho(t) e_l^\dagger g_n, \tag{31}$$

$$\mathcal{J}\rho(t) = 2 \sum_{l,n} \Gamma_{nl}^{\rm sp} g_n^\dagger e_l \rho(t) e_l^\dagger g_n, \tag{32}$$

where

$$\Gamma_{nl}^{\rm sp} = \gamma \int {\rm d}\phi \int {\rm d}\theta \sin\theta \mathcal{W}(\theta,\phi) |\eta_{ln}(\mathbf{k})|^2. \tag{33}$$

The repumping pulses have constant amplitude and duration $\tau_{\rm sp}$ long enough to depopulate totally the excited states. On the other hand, remember that (collective) spontaneous emission rates in the Festina Lente limit are small in comparison to the trap frequency [16]. We can formally integrate equation (30), to obtain that after the spontaneous emission step (*i.e.* for $\tau_{\rm sp}$ sufficiently long):

$$\rho(t+\tau_{\rm abs}+\tau_{\rm sp}) = \rho(t) - \sum_{lm} \Gamma_{lm}^{\rm abs} \left[g_m^\dagger g_m \rho(t) + \rho(t) g_m^\dagger g_m\right] + 4 \int_0^\infty {\rm d}\tau \sum_{mnl} \Big[\Gamma_{ln}^{\rm sp} \Gamma_{lm}^{\rm abs} g_n^\dagger {\rm e}^{-\sum_k \Gamma_{kl}^{\rm sp} g_k g_k^\dagger \tau} g_m \rho(t) \times g_m^\dagger {\rm e}^{-\sum_k \Gamma_{kl}^{\rm sp} g_k g_k^\dagger \tau} g_n\Big], \tag{34}$$

where we have employed the fact that at time t all the atoms are in the ground state. Note, that if $\hat{H}_{\rm eff}$ in equation (31) contained a contribution of $\hat{H}_{\rm dip}$ (real part of the dipole-dipole interactions), such contributions would exactly cancel out in RWA in expression (34), provided $\rho(t+\tau_{\rm abs})$ remained diagonal in the Fock representation.

Equation (34) describes the full cooling cycle, *i.e.* maps the diagonal $\rho(t)$ with all atoms in ground state into the diagonal $\rho(t+\tau_{\rm abs}+\tau_{\rm sp})$ with all atoms again in the ground state. The last term in the above equation describes the integral over all possible times τ in which the quantum jump from the excited state l to the ground state n occurs. The amplitude of the excited state is damped during the time τ with the collective rate $\sum_k \Gamma_{kl}^{\rm sp} g_k g_k^\dagger$, which evidently contain Bose enhancement factors, *i.e.* is proportional to occupation numbers plus one of the corresponding occupations of the ground trap levels.

By applying the annihilation and creation operators to the initial ground Fock density matrix, and by time integrating, one calculates easily the probability of one atom to jump from an initial state n to a final state m, obtaining the rate equation:

$$\dot{N}_n = \sum_m \Gamma_{n\leftarrow m} N_m - \sum_m \Gamma_{m\leftarrow n} N_n \tag{35}$$

with

$$\Gamma_{n\leftarrow m} = \sum_l \frac{2\Gamma_{lm}^{\rm abs} \Gamma_{nl}^{\rm sp} (N_n + 1 - \delta_{n,m})}{\sum_{n'} \Gamma_{n'l}^{\rm sp} (N_{n'} + 1 - \delta_{n',m})}\,. \tag{36}$$

Observe that these rates are considerably different compared to those described by equation (16). In particular, although the spontaneous emission is, at it should, still collective, the broadening of the absorption resonance is not present here, because the absorption is not affected by the spontaneous emission. This effect is the main advantage of the present model. In particular Ω is not restricted to be smaller than 2γ, and that allows the cooling process to be very much faster.

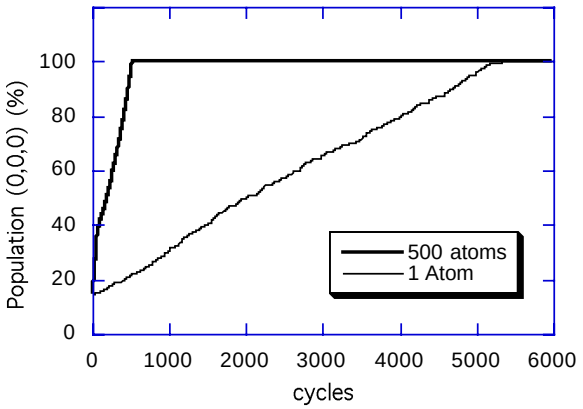

Fig. 7. Condensation dynamics into $(0,0,0)$, for $\eta = 2.0$ and a sequence of pulses of detunings $s = -12$, -6, -4, 0, -13, -7, -5, -1. For all the pulses $A_{x,y,z} = 1$ except for $s = 0$ for which $A_z = -2$. The initial distribution is thermal with mean $\langle n \rangle = 6$. Dotted and solid lines represent respectively the case of $N = 1$ and 500 atoms.

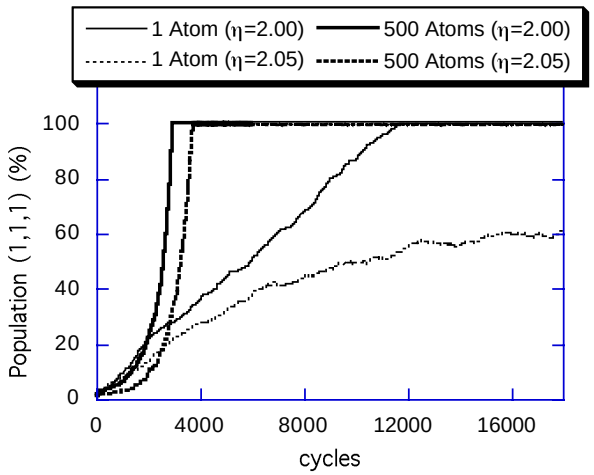

Fig. 8. Condensation dynamics into $(1,1,1)$, using a sequence of pulses of detunings $s = -12$, -6, -3, 3, -13, -7, -4, -2. For all the pulses $A_{x,y,z} = 1$. The initial distribution is thermal with mean $\langle n \rangle = 6$. We have depicted with different dashes and thickness for $\eta = 2.0$ and 2.05, the cases of $N = 1$ and 500 atoms

6 Two-step model: Numerical results

Rate equations (35) can be simply simulated using standard Monte-Carlo procedures. We have performed such simulations for $N = 1$ up to $N = 500$ atoms, in various dimensions, and for various cooling strategies. Franck-Condon factors and trap frequencies have been approximated using the states of an isotropic trap with frequency ω. We concentrate here on 3-dimensional cooling. As in the previous cooling model of [17] and the first sections of this paper, we consider the cooling beyond the Lamb-Dicke limit, *i.e.* for traps for which the Lamb-Dicke parameter $\eta = \sqrt{E_{\rm R}/\hbar\omega}$ is larger than one. We consider three Raman transitions induced by laser pairs propagating in directions x, y, and z characterized by three different effective Rabi frequencies $\Omega_0 f(t) A_j$, where $A_{j=x,y,z}$ account for difference of intensities or dephasing between the lasers. It is easy to observe from the form of the rates, and the expression for $\Gamma^{\rm abs}_{lm}$, that the same dark-state mechanisms as those discussed in reference [17] can be applied in the new model, *i.e.* "Franck-Condon"-dark-states, and "interference"-dark-states. In the following we shall apply these dark-state techniques to condense into different states of the trap.

In Figure 7 we present our result for ground state cooling of 1 and 500 sodium atoms in a three-dimensional trap with a Lamb-Dicke parameter $\eta = 2$, using 20 three-dimensional energy shells (*i.e.* 1771 trap levels) for the calculation. The initial state of the system corresponds to mean energy $6\hbar\omega$, and is the same for all the rest of the figures of this paper. The pulse sequence is $s = -12$, -6, -4, 0, -13, -7, -5, -1. $A_{x,y,z} = 1$, except for $s = 0$, for which $A_{x,y} = 1, A_z = -2$. Pulses 1 and 5 are confining, 2, 3, 6 and 7 pseudo-confining, and 4 and 8 are dark-state cooling pulses for $(0,0,0)$. As in the previous sections the many body effects introduce one very important element to the dynamics: the bosonic-enhancement factors, that speed up the dynamics enormously. The time scale is such that each cooling cycle must be longer than $2\pi/\omega \simeq 10^{-4}$ s. In such a case, the function $\tilde{f}$ can be taken to be sufficiently narrow to neglect non-resonant transitions. Therefore 1000 cycles of cooling correspond to about one second. Cooling of one atom requires here few seconds, whereas collective cooling takes about 0.1 s. After achieving condensation with 500 atoms, confining pulses can be avoided, a single dark state pulse can keep the atoms in the condensed state.

In Figure 8 we show results for cooling into the state $(1,1,1)$ using the sequence $s = -12$, -6, -3, 3, -13, 7, -4, -2, with $A_{x,y,z} = 1$. Here the pulse 4 is a "Franck-Condon"-dark-state pulse ($\eta^2 = s+1$), the other are either confining or auxiliary. First, note that when dark state condition is fulfilled exactly ($\eta = 2$), cooling of a single atom to $(1,1,1)$, although slow, is possible. This cooling mechanism is, however, very fragile. A tiny perturbation of the dark state ($\eta = 2.05$) makes efficient cooling impossible. This conclusion does not hold for many atoms though. As in the previous section, quantum statistics helps to achieve 100% condensation that is robust with respect to parameter changes; the results for $\eta = 2$ or 2.05 are almost indistinguishable, the cooling time is much shorter than in the 1 atom case, and takes about 1 s.

7 Conclusions

In this paper we have analysed the dynamical cooling scheme, originally designed for single-atoms, for the case of N identical bosons in the trap. We have presented the quantum master equation which describes the dynamics of the system. We have adiabatically eliminated the excited states to obtain a set of rate equations. The many-atom rates are non-linear respect to the occupation numbers of each trap level. In particular two new effects appear: bosonic-enhancement factors, and collective spontaneous emission rates. We have analysed the new statistical

effects in comparison with the single-atom case, and concluded that for the many-atom case the dark-state conditions are more robust due to the bosonic enhancement. We have also studied the differences between one- and two-dimensional problems. Finally, we have presented a different model of cooling in which the absorption and spontaneous processes occur separately and consecutively. We have developed the proper master equation (using coarse graining in time), and developed new rate equations. This new cooling method, which in fact is usually realized in experiments on Raman cooling, proves to solve several problems inherent to the first model. Using Monte-Carlo simulations we have demonstrated that the condensation into an arbitrary state of the trap is possible, robust, and can be achieved in experimentally feasible traps. It is typically accompanied by multistability and hysteresis phenomena which will be discussed in detail elsewhere [19].

We have neglected in our approach atom-atom collisions. We do not think that collisions will change the picture presented here essentially. Atom-atom interaction will make effective energy levels in the trap non-harmonic. Most probably, broader or chirped absorption pulses will have to be used to assure efficient population transfers. Collisionally induced population redistribution should not affect condensate in the (collisionally modified) ground state $(0,0,0)$, since this state corresponds to thermal equilibrium at very low temperatures. Thermalisation mechanism might destroy condensates in excited states, but that will depend on time scales. Condensation requires according to our calculation seconds, but we have not attempted to optimize this time; 10 times shorter condensation times are thus presumably feasible. Such times become shorter than thermalisation time due to collisions if N is not too large, and η not too small.

We acknowledge fruitful discussions with J.I. Cirac. Partial support from the Spanish Dirección General de Investigación Científica y técnica (Grant No. PB95-0955) and from the Junta de Castilla y León (Grant No. SA 16/98) is acknowledged. This work has been supported by the EU through the TMR network ERBXTCT96-0002, and by the Deutsche Forschungsgemeinschaft under SFB 407.

Appendix A: Developing of the master equation of the first model

We treat the vacuum electromagnetic modes as a reservoir (R), whereas the trapped atoms are called the system (S) [27]. A global density operator $\chi(t)$ describes the state of the system plus reservoir (S$\oplus$R). We define the reduced density operator $\rho(t)$ for the system S as the trace of χ over the reservoir degrees of freedom:

$$\rho(t) = \mathrm{tr}_{\mathrm{R}}[\chi(t)]. \tag{A.1}$$

Our purpose in this appendix is to obtain an expression for $\dot{\rho}(t)$ from the equation for $\dot{\chi}(t)$ after tracing over R. The dynamics of χ is given by the von Neumann equation, which in the interaction picture with respect to free evolution of atoms and vacuum electromagnetic modes, takes the form:

$$\dot{\tilde{\chi}}(t) = -\mathrm{i}[\tilde{H}_{\mathrm{las}}(t), \tilde{\chi}(t)] - \mathrm{i}[\tilde{H}_{\mathrm{af}}(t), \tilde{\chi}(t)], \tag{A.2}$$

where the atom-vacuum interaction Hamiltonian has the form

$$\tilde{H}_{\mathrm{af}}(t) = -\mathrm{i}\sum_{l,m}\sum_{\mu}\int d^3\mathbf{k}\sqrt{\frac{k}{2\epsilon_0(2\pi)^3}}(\mathbf{d}\cdot\boldsymbol{\epsilon}_{\mathbf{k}\mu}) \times \eta_{lm}(\mathbf{k}) e_l^{\dagger} g_m a_{\mathbf{k}\mu} \mathrm{e}^{i(\omega_l^{\mathrm{e}}-\omega_m^{\mathrm{g}}-\omega(k))} + h.c. \tag{A.3}$$

where $a_{\mathbf{k}\mu}$, $a_{\mathbf{k}\mu}^{\dagger}$ are the annihilation and creation operators of a photon mode characterised by a wavevector $\mathbf{k}$, frequency $\omega(k)$, and a polarisation μ, with polarisation vector $\boldsymbol{\epsilon}_{\mathbf{k}\mu}$; $\mathbf{d}$ denotes the atomic dipole vector characterising the consider electronic transition.

Integrating equation (A.2) and substituting in the second commutator in equation (A.2):

$$\begin{aligned}\dot{\tilde{\chi}}(t) = &-\mathrm{i}[\tilde{H}_{\mathrm{las}}(t), \tilde{\chi}(t)] - \mathrm{i}[\tilde{H}_{\mathrm{af}}(t), \chi(0)] \\ &- \int_0^t \mathrm{d}t' \big[\tilde{H}_{\mathrm{las}}(t), [\tilde{H}_{\mathrm{af}}(t'), \tilde{\chi}(t')]\big] \\ &- \int_0^t \mathrm{d}t' \big[\tilde{H}_{\mathrm{af}}(t), [\tilde{H}_{\mathrm{af}}(t'), \tilde{\chi}(t')]\big].\end{aligned} \tag{A.4}$$

Up to this point the equation is exact, but quite intractable. Some reasonable approximations are needed:

- the interaction time is assumed to be turned on at $t = 0$. At that time no correlation exists between S and R. Then $\chi(0) = \rho(0)R_0$, where R_0 is an initial reservoir density operator l;
- tracing equation (A.4) respect to the reservoir, we obtain:

$$\begin{aligned}\dot{\tilde{\rho}}(t) = &-\mathrm{i}[\tilde{H}_{\mathrm{las}}(t), \tilde{\rho}(t)] \\ &- \int_0^t \mathrm{d}t' \mathrm{tr}_{\mathrm{R}}\Big\{\big[\tilde{H}_{\mathrm{las}}(t), [\tilde{H}_{\mathrm{af}}(t'), \tilde{\chi}(t')]\big]\Big\} \\ &- \int_0^t \mathrm{d}t' \mathrm{tr}_{\mathrm{R}}\Big\{\big[\tilde{H}_{\mathrm{af}}(t), [\tilde{H}_{\mathrm{af}}(t'), \tilde{\chi}(t')]\big]\Big\},\end{aligned} \tag{A.5}$$

  where we have assumed $\mathrm{tr}_{\mathrm{R}}\{\tilde{H}_{\mathrm{af}}(t), R_0\} = 0$ (which can always be done [27]);
- since the coupling H_{af} between S and R is assumed to be very weak, and since R is a very large system virtually unaffected by its coupling to S, we can extend the initial factorization to any other time: $\tilde{\chi}(t) = \tilde{\rho}(t)R_0$. This is the so-called Born approximation;
- in order to trace over the reservoir variables, we will assume a vacuum statistics of the reservoir, this means that $\langle a_{\mathbf{k}\mu}^{\dagger} a_{\mathbf{k}'\mu'}^{\dagger}\rangle = \langle a_{\mathbf{k}\mu} a_{\mathbf{k}'\mu'}\rangle = \langle a_{\mathbf{k}\mu}^{\dagger} a_{\mathbf{k}'\mu'}\rangle = 0$, $\langle a_{\mathbf{k}\mu} a_{\mathbf{k}'\mu'}^{\dagger}\rangle = \delta(\mathbf{k}-\mathbf{k}')\delta_{\mu\mu'}$. Also $\langle a_{\mathbf{k}\mu}\rangle = \langle a_{\mathbf{k}\mu}^{\dagger}\rangle = 0$,

and therefore the second term in the RHS of equation (A.5) vanishes:

$$\dot{\tilde{\rho}}(t) = -\mathrm{i}[\tilde{H}_{\mathrm{las}}(t), \tilde{\rho}(t)] - \int_0^t \mathrm{d}t' \mathrm{tr}_{\mathrm{R}} \Big\{ \big[\tilde{H}_{\mathrm{af}}(t), [\tilde{H}_{\mathrm{af}}(t'), \tilde{\rho}(t') R_0]\big] \Big\}; \tag{A.6}$$

- Markov approximation: the decay of the reservoir correlation functions is assumed to be very much faster than the typical time scales for the system dynamics, and therefore $\rho(t)$ changes insignificantly over the time taken for the correlation functions to vanish. Then we can approximate in equation (A.6) $\rho(t') \to \rho(t)$ and $\int_0^t \to \int_0^\infty$, obtaining the ME in the Born-Markov approximation:

$$\dot{\tilde{\rho}}(t) = -\mathrm{i}[\tilde{H}_{\mathrm{las}}(t), \tilde{\rho}(t)] - \int_0^\infty \mathrm{d}t' \mathrm{tr}_{\mathrm{R}} \Big\{ \big[\tilde{H}_{\mathrm{af}}(t), [\tilde{H}_{\mathrm{af}}(t'), \tilde{\rho}(t) R_0]\big] \Big\}. \tag{A.7}$$

In our case the Born-Markov approximation is valid, since the characteristic frequency scales fulfill $N\gamma$, Ω, ω, $|\delta| \ll \omega_{\mathrm{L}}$, ω_0, c/L, where L is the typical dimension of the atomic sample. After some calculation one obtains equation (3) using the vacuum statistics.

References

1. S. Chu, Nobel Lecture, Rev. Mod. Phys. **70**, 685 (1998); C. Cohen-Tannoudji, Nobel Lecture, *ibid.*, 707; W.D. Phillips, Nobel Lecture, *ibid.*, 721.
2. M.H. Anderson, J.R. Ensher, M.R. Matthews, C.E. Wieman, E.A. Cornell, Science **269**, 198 (1995); K.B. Davis, M.O. Mewes, M.R. Andrews, N.J. van Drutten, D.S. Durfee, D.M. Kurn, W. Ketterle, Phys. Rev. Lett. **75**, 3969 (1995); C.C. Bradley, C.A. Sackett, R.G. Hulet, *ibid.* **78**, 985 (1997).
3. C.J. Myatt, E.A. Burt, R.W. Ghrist, E.A. Cornell, C.E. Wieman, Phys. Rev. Lett. **78**, 586 (1997).
4. D. Boiron, A. Michaud, P. Lemonde, Y. Castin, C. Salomon, S. Weyers, K. Szymaniec, L. Cognet, A. Clairon, Phys. Rev. A **53**, R3734 (1996).
5. M. Rauner, M. Schiffer, S. Kuppens, G. Wokurka, G. Birkl, K. Sengstock, W. Ertmer, in *Laser Spectroscopy XIII* (Springer-Verlag, Heidelberg, 1997).
6. T. Müller-Seydlitz, M. Hartl, B. Breyger, H. Hansel, C. Keller, A. Schnetz, R.J.C. Spreeuw, T. Pfau, J. Mlynek, Phys. Rev. Lett. **78**, 1038 (1997).
7. A. Aspect, E. Arimondo, R. Kaiser, N. Vanteenkiste, C. Cohen-Tannoudji, Phys. Rev. Lett. **61**, 826 (1988).
8. M. Kasevich, S. Chu, Phys. Rev. Lett. **69**, 1741 (1992).
9. E. Arimondo, G. Orriols, Lett. Nuovo Cimento **17**, 333 (1976).
10. D.W. Sesko, T.G. Walker, C.E. Wieman, J. Opt. Soc. Am. B **8**, 946 (1991).
11. M. Olshan'ii, Y. Castin, J. Dalibard, *Proc. 12th Int. Conf. on Laser Spectroscopy*, edited by M. Inguscio, M. Allegrini, A. Lasso (World Scientific, Singapour, 1996).
12. A.M. Smith, K. Burnett, J. Opt. Soc. Am. B **9**, 1256 (1992).
13. K. Ellinger, J. Cooper, P. Zoller, Phys. Rev. A **49**, 3909 (1994).
14. U. Janicke, M. Wilkens, Europhys. Lett. **35**, 561 (1996)
15. Y. Castin, J.I. Cirac, M. Lewenstein, Phys. Rev. Lett. **80**, 5305 (1998).
16. J.I. Cirac, M. Lewenstein, P. Zoller, Europhys. Lett. **35**, 647 (1996).
17. L. Santos, M. Lewenstein, Phys. Rev. A (in print).
18. G. Morigi, J.I. Cirac, M. Lewenstein, P. Zoller, Europhys. Lett. **39**, 13 (1997).
19. L. Santos, M. Lewenstein, J.I. Cirac, Y. Castin, Phys. Rev. Lett. (submitted).
20. I. Marzoli, J.I. Cirac, R. Blatt, P. Zoller, Phys. Rev. A **49**, 2771 (1994).
21. M. Lewenstein, L. You, J. Cooper, K. Burnett, Phys. Rev. A **50**, 2207 (1994).
22. M. Lewenstein, L. You, Adv. At. Mol. Opt. Phys. **36**, 221 (1996).
23. E. Tiesinga, A.J. Moerdijk, B.J. Verhaar, H.T.C. Stoof, Phys. Rev. A **46**, R1167 (1992).
24. J.I. Cirac, M. Lewenstein, P. Zoller, Phys. Rev. A **50**, 3409 (1994).
25. C.W. Gardiner, *Handbook of Stochastical Methods* (Springer-Verlag, 1985).
26. C.W. Gardiner, *Quantum Noise* (Springer-Verlag, Berlin, 1991).
27. H. Carmichael, *An Open Systems Approach to Quantum Optics* (Springer-Verlag, 1993).
28. J.I. Cirac, M. Lewenstein, P. Zoller, Phys. Rev. A **51**, 5899 (1995).
29. G. Lenz, P. Meystre, E.M. Wright, Phys. Rev. A **50**, 1681 (1994); M.G. Moore, P. Meystre, Phys. Rev. A **56**, 2989 (1997).
30. R.H. Dicke, Phys. Rev. A **93**, 99 (1954).